Streamlining Information Transfer between Construction and Structural Engineering
Edited by Shiau, J., Vimonsatit, V., Yazdani, S., and Singh, A.

ISBN: 978-0-9960437-7-9

EXPERIMENTAL STUDY OF INNOVATIVE COMPOSITE BUCKLING-RESTRAINED FUSE FOR CONCENTRICALLY BRACED FRAMES UNDER CYCLIC LOAD

MASOUD MOHAMMADI[1, 2], MOHAMMAD ALI KAFI[1], ALI KHEYRODDIN[1], HAMID REZA RONAGH[2]

[1]*Dept of Civil Engineering, Semnan University, Semnan, Iran*
[2]*Centre for Infrastructure Engineering, Western Sydney University, Sydney, Australia*

Concentrically Braced Frames (CBFs) are among the most commonly used lateral resisting systems utilized in the construction of steel structures due to their rigidity, low lateral displacement and ease of implementation. However, the lack of ductility due to the buckling that occurs in the bracing elements before yielding is their main disadvantage. This study presents an innovative Composite Buckling Restrained Fuse (CBRF) to be used as a bracing segment in concentrically braced frames that improves the ductility and eliminates premature buckling. The proposed CBRF with relatively small dimensions is a hysteretic damper consisting of thin steel plate core and extra tensile elements embedded in a composite encasement. Two CBRF samples are designed and tested experimentally. The results indicate that the proposed structural fuse has a ductile behaviour with high energy absorption and sufficient strength along with a reasonably stable hysteretic response under cyclic load.

Keywords: Steel structure, Structural fuse, Ductility.

1 INTRODUCTION

Concentrically Braced Frames (CBFs) have become prevalent as a lateral load resisting system over the last three decades. Large lateral stiffness, low lateral displacement associated with ease of implementation at a low-cost are the advantages of the CBFs which encourages the increasing use of this system in construction. However, damage of the whole brace as a result of buckling have been frequently reported under severe lateral loads. In many instances such as Northridge earthquake in 1994, buckling of the whole brace before yielding was the main problem reported of this lateral system which limited the ductility and affected the energy dissipation capacity of the frame (Bruneau *et al.* 2011) and collapse propagation (Mohajeri Nav *et al.* 2017, Abbasnia *et al.* 2016). Many studies since have been focused on increasing the ductility of CBFs. In most of these studies, researchers tried to make a modification in connections of the brace or placed a ductile member as a hysteretic damper into the brace to increase the deformation capacity of the system. Among these, sliding friction mechanism dampers and connections (Mualla and Belev 2002, Rodgers *et al.* 2017) and yielding parts such as T-shaped dampers (TahamouliRoudsari *et al.* 2018) and ring element fuses (Andalib *et al.* 2018, Deihim and Kafi 2017) can be named. From a different perspective, some of the researchers were looking at methods to prevent premature buckling of the braces. Confining braces by mortar encase and steel cases were some of the techniques gradually implemented till the modern Buckling Restrained Braces (BRBs) were evolved (Xie 2005).

The current study aims to present an innovative Composite Buckling Restrained Fuse (CBRF) to be used as sacrificial brace segment. CBRF with relatively small dimensions is a hysteretic damper with different tension and compression capacity. Extra tensile elements have been used innovatively so that no reduction of the tensile capacity occurs unlike what happens when an ordinary fuse is used. In this paper, the experimental results on the proposed CBRF are described, and the results are presented.

2 GENERAL DESCRIPTION OF CBRF AND INNOVATIVE TENSILE ELEMENT

Structural fuses are the sacrificial yielding elements embedded in different parts of a structure such as braces, beams or columns, depending upon their bearing load type, to absorb the energy of the loads exerted to the system. CBRF proposed in this paper is a kind of replaceable axial structural fuse with a short length. This fuse comprised tensile elements and thin steel core plate restrained in a composite encase. This reduced length BRB is placed at each end of the bracing members, with different tension and compressive capacity, to localise the structural failures and dissipate the energy of a severe load. Figure 1, illustrates CBRF components and its placement in a diagonal bracing frame.

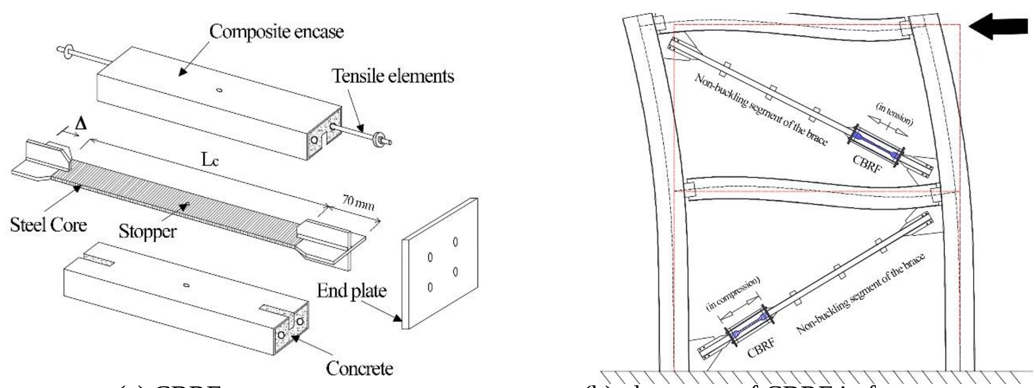

(a) CBRF components (b) placement of CBRF in frame

Figure 1. CBRF assemblage and placement.

Assume that the frame, shown in Figure 1(b) without any fuse, is subjected to an severe lateral load. Depending on the force, one of the braces might be under tension while the other may buckle under compression. Utilizing an ordinary fuse in each bracing member causes these elements to fail prior to any other segments allowing the dissipation of energy. These sacrificial elements which have almost the same tensile and compressive capacity are designed based on the critical compressive load of the bracing members to prevent the premature buckling by considering a reduction factor. Since the bracing member has different tensile and compressive capacity, this leads that limitation happens in both tension and compression capacity of the bracing member and reduces the total lateral bearing capacity of the frame. In the proposed CBRF the tensile capacity is designable. Extra tensile elements, steel bars, have been used innovatively so that no limitation of the tensile capacity of the whole brace occurs.

3 DESIGNING AND DETAILING OF CBRF

The cross-sectional area of the steel core, A_C, is designed based on the method mentioned in AISC 341 (AISC 2016) by considering a reduction factor, ϕ, which depends on the compressive strength of fuse, β, the average strain hardening of the steel core, ω, and the expected yield stress, R_y, for the core plate section, Eq. (1).

$$\phi \leq \frac{1}{\beta \omega R_y} \tag{1}$$

Moreover, Tensile elements can be designed based on the desired maximum tensile force that would occur in the whole bracing member upon the anticipated story drift. Determining the optimal length of CBRF is another essential parameter that plays an important role in absorbing the energy and plastic behavior of the fuse. Due to the short length of CBRF, at the same displacement, Δ, the core average strain, $\varepsilon_c=\Delta/L_c$, would be more than the similar longer ones. From the practical metallurgical point of view, according to the protocol of loading and number of inelastic cycles, the minimum length of the core plate, L_c, can be evaluated based on preventing the fracture due to low-cyclic fatigue phenomena (Mirtaheri *et al.* 2011), Eq (2).

$$L_c \geq \left(\frac{1}{\varepsilon_c'}\right) \times \lambda^{|c|} \tag{2}$$

Where, ε_c' is the real ultimate strain for steel material, c is the fatigue ductility exponent and for λ we have:

$$\lambda = \sum_{1}^{m} \left(2n_i \times \Delta_i^{\left|\frac{1}{c}\right|}\right) \tag{3}$$

Where m is the total number of in-elastic cycles of loading protocol and n_i is the number of cycles with the same amplitude cycle of Δ_i.

4 EXPERIMENTAL STUDY

In order to investigate the performance of CBRF and the effect of extra tensile elements, an experimental program was conducted. Two specimens were designed and tested subjected to cyclic loads. The specimen 1, was a Reduced Length Buckling Restrained Braces, RL-BRB, without the tensile bar unlike specimen 2 which contained the tensile bar.

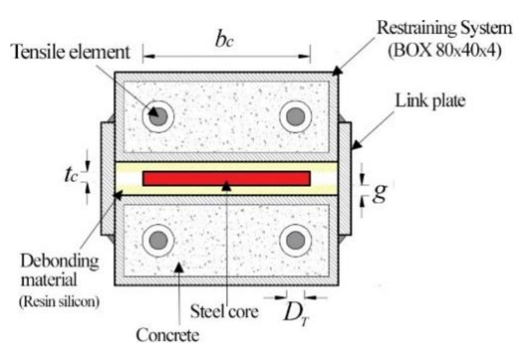

Figure 2. CBRF cross-section.

Steel with the yield stress of 290 MPA and ultimate stress of 400 MPA at the strain of 0.25% was used for the core steel plate. Considering the critical load of 120kN for a diagonal bracing member and employing the safety factor of 0.5, the cross-sectional area of the core, A_c, was obtained to be 2.1 cm^2. The composite encase was made of two steel box filled with normal concrete connected by two steel link plates. 2mm gap size was considered for the free space between the core and the composite encase, shown in Figure 2. Length of the core plate, L_c, was calculated as 30cm based on the Eq. (2) as discussed in Section 4.1. Specimen parameters are summarized in Table 1. The t_c and b_c are the thickness and the width of core plate and g is the gap size.

Table 1. Specimen parameters.

No.	Specimens	Core Plate			Restraining system	Tensile bars
		L_c (mm)	t_c (mm)	b_c (mm)	g (mm)	D_T (mm)
1	RL-BRB	300	5	42	2	-
2	$B_{co}L_3D_8$	300	5	42	2	8

4.1 Loading Protocol

ATC24 loading protocol was utilized for evaluating the cyclic performance of the specimens. This loading protocol includes cycles which are a multiplier of the yield deformation, Δ_y, of the segment that was calculated based on the material properties (Krawinkler 1992). The slow and manageable rate of deterioration in this loading protocol allows prediction of the load-deformation response with more confidence without any missing cycles. At the beginning of the loading protocol, nine cycles of the loading were considered with the elastic amplitude lower than Δ_y to measure the initial axial stiffness of the specimen. The subsequent inelastic phase of the loading was a set of variable deformation amplitude gradually increasing by multipliers of Δ_y at 2, 3, 4, 6, 8, 11, 14, 18, 22, 27, 32, 38 times, which follow a geometric progression. The optimized length of the fuse was calculated based on the Eq. (2) as $L_c \geq 25.1$ cm. In order to avoid the anticipated fracture due to low-cyclic fatigue phenomena, core length was taken $L_c = 30$ cm for the specimens.

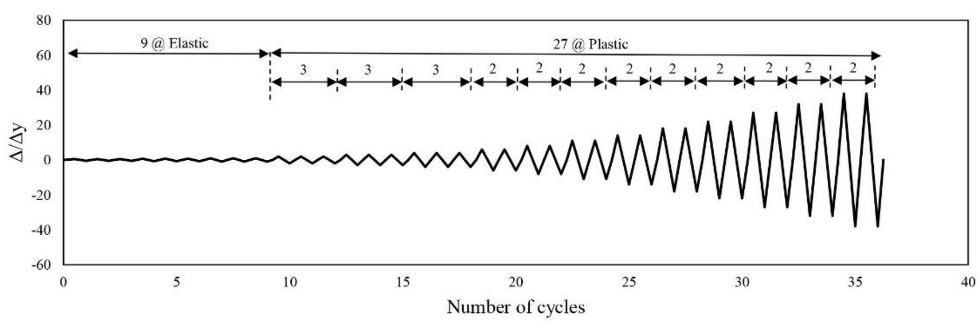

Figure 3. Loading protocol (Krawinkler 1992).

4.2 Test Setup

The uniaxial test setup composed of a hydraulic jack capable of exerting cyclically up to a maximum of 2000kN compressive load and a maximum of 1000kN tensile load while accommodating a maximum stroke of ±100 mm. It was also equipped with a 1000kN load-cell. As shown in Figure 4, the setup consisted of two reaction blocks which were connected to the strong floor. One end of the specimens was attached to the reaction block, whereas the other end was connected to the hydraulic actuator. Linear guideways (wagons) were used in the setup to prevent the lateral displacement of the load-cell during the test and exert the load axially to the specimen without rotation. Two displacement-control linear LVDTs with high accuracy were mounted on the load support to monitor the exact displacement. Moreover, two other LVDTs were placed on the composite encase of the specimen. Figure 4 depicts the assembled CBRF specimen in the setup.

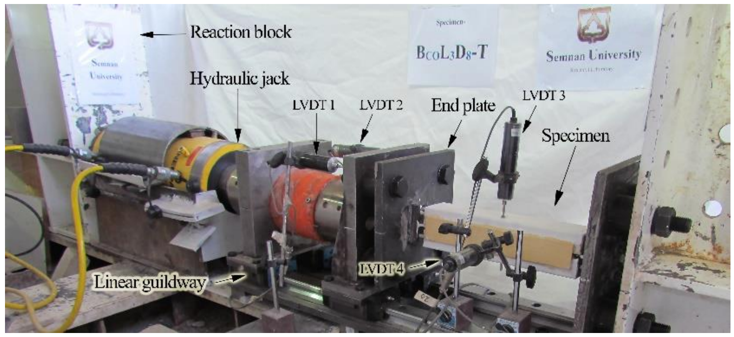

Figure 4. Assembled CBRF specimen in the setup.

5 EXPERIMENTS AND RESULTS

The hysteresis curves of the two specimens that were mentioned in Table 1 are presented in Figure 5, where the failure point of each specimen is marked with a red triangle and the envelope curves are depicted by the dashed line.

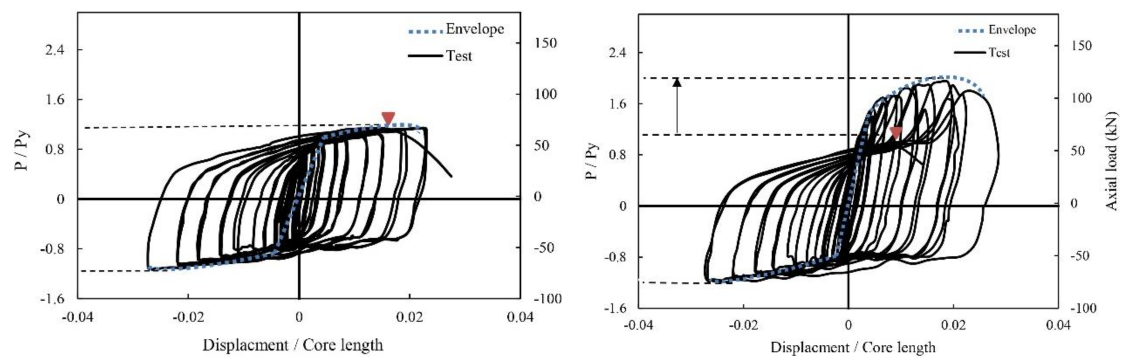

(a) Specimen 1, RL-BRB

(b) Specimen 2, $B_{co}L_3D_8$-T

Figure 5. The hysteretic response of specimens.

The hysteresis results of two specimens were investigated closely. The RL-BRB, specimen 1, was the control sample to compare the performance of using extra tensile elements in the fuse. As shown in Figure 5(a), the hysteretic loops of the specimen 1 are steady and stable without pinching. The fuse has almost the same bearing capacity in the compression and tension and the ductility is improved. Passing through the critical load of the core and occurrence of buckling in the first mode, the composite encase prevents the early global buckling of the central core and leads the core to reach higher modes as it displaces axially. The sawtooth parts of the curves show the resulting degradation due to the progress of the bucking modes in compression phase. The detected differences between the compression and the tension load bearing ratio are not impressive in the specimen 1. The maximum axial bearing ratios of the RL-BRB are P_{max} / P_y=1.14 in tension and 1.13 in compression. The elastic stiffness of RL-BRB obtained from the initial elastic cycles is about 113 kN/mm. The maximum inelastic axial average core strain after the end of 32 cycles at the failure point is 3.4%, which is interpreted by the appropriate behaviour of the core in ductility and energy dissipation. As shown in Figure 5(b), the hysteresis curve of the CBRF demonstrate the steady stable wide loops similar to Specimen which is a desirable improvement on the tensile strength and energy dissipation for the CBRF. The maximum axial compressive bearing ratio of the CBRF is about 1.15 which is almost the same as that in Specimen 1. In addition, The maximum tensile bearing ratio is 1.94 (axial load of 120kN) due to the utilisation of the extra tensile bars. The elastic stiffness of the CBRF obtained from the initial elastic cycles as 110 kN/mm and the maximum inelastic axial average core strain after the end of 32 cycles at the failure point is about 3.4%, which are almost similar to those of Specimen 1.

6 CONCLUSION

This study presents an innovative structural fuse, CBRF, to be used as a segment in the concentric braces. This kind of replaceable hysteresis damper, with different capacity in tension and compression, has the ability to compensate the limitation of the tensile capacity unlike what occurs when an ordinary fuse is used in a bracing member. Two specimens were tested experimentally. The results indicate that CBRF offers favourable improvement in the tensile capacity and energy dissipation along with reasonably stable hysteretic response under cyclic loads.

References

Abbasnia, R., Mohajeri Nav, F.,Usefi, N., and Rashidian, O., A New Method for Progressive Collapse Analysis of RC Frames, *Structural Engineering and Mechanics*, 60(1), 31-50, 2016.

AISC. *ANSI/AISC 341-16, Seismic Provisions for Structural Steel Buildings*, United States of America, Chicago: American Institute Of Steel Construction, 2016.

Andalib, Z., Kafi, M. A., Bazzaz, M., and Momenzadeh, S., Numerical Evaluation of Ductility and Energy Absorption of Steel Rings Constructed from Plates, *Engineering Structures,* 169, 94-106, 2018.

Bruneau, M., Uang, C. M., and Sabelli, R., *Ductile Design of Steel Structures, 2nd Edition*, McGraw-Hill, 2011.

Deihim, M. and Kafi, M. A., A Parametric Study into the New Design of a Steel Energy-Absorbing Connection, *Engineering Structures,* 145, 22-33, 2017.

Krawinkler, H., *ATC24, Guidelines for Cyclic Seismic Testing of Components of Steel Structures*, Applied Technology Council, Redwood City, California, 1992.

Mirtaheri, M., Gheidi, A., Zandi, A. P., Alanjari, P., and Samani, H. R., Experimental Optimization Studies on Steel Core Lengths in Buckling Restrained Braces, *Journal of Constructional Steel Research*, 67(8)**,** 1244-1253, 2011.

Mohajeri Nav, F., Usefi, N., and Abbasnia, R., Analytical Investigation of Reinforced Concrete Frames Under Middle Column Removal Scenario, *Advances in Structural Engineering,* 2017.

Mualla, I. H. and Belev, B., Performance of Steel Frames with w New Friction Damper Device Under Earthquake Excitation, *Engineering Structures*, 24(3)**,** 365-371, 2002.

Rodgers, G. W., Chase, J. G., Causse, R., Chanchi, J., and MacRae, G. A., Performance and Degradation of Sliding Steel Friction Connections: Impact of Velocity, Corrosion Coating and Shim Material, *Engineering Structures,* 141, 292-302, 2017.

TahamouliRoudsari, M., Eslamimanesh, M. B., Entezari, A. R., Noori, O., and Torkaman, M., Experimental Assessment of Retrofitting RC Moment Resisting Frames with ADAS and TADAS Yielding Dampers. *Structures,* 14, 75-87, 2018.

Xie, Q., State of the Art Of Buckling-Restrained Braces in Asia, *Journal of Constructional Steel Research*, 61(6)**,** 727-748, 2005.